Microchimica Acta (2021) 188: 146
https://doi.org/10.1007/s00604-021-04798-x

SHORT COMMUNICATION

A serotonin voltammetric biosensor composed of carbon nanocomposites and DNA aptamer

Jingjing Li[1] · Yunpei Si[1] · Yae Eun Park[2] · Jung-Seok Choi[3] · Sung Mi Jung[4] · Ji Eun Lee[2] · Hye Jin Lee[1]

Received: 21 January 2021 / Accepted: 19 March 2021 / Published online: 1 April 2021

Abstract

A sensitive and selective voltammetric biosensor composed of layer-by-layer (LbL) self-assembly of positively charged poly(diallyldimethylammonium)-wrapped oxidized single-walled carbon nanotubes (PDDA-oSWCNTs), negatively charged serotonin (5-hydroxytryptamine, 5-HT)-specific aptamer, and tyrosinase on Au nanoparticles deposited screen printed carbon electrode was developed for measurement of 5-HT. Surface characteristics of 5-HT biosensor were explored using scanning electron microscopy, X-ray photoelectron spectroscopy, and electrochemical impedance spectroscopy. The respective effects of 5-HT-specific aptamer and oSWCNTs on the detection of 5-HT were investigated by differential pulse voltammetry (DPV). The peak current at the potential of 0.29 V (vs. Ag/AgCl) increased with respect to 5-HT concentration resulting in two dynamic ranges from 0.05 to 0.5 and 1 to 20 μM with a limit of detection of 2 nM from the LbL biosensor in buffer solution, which were better than those without the LbL of aptamer and oSWCNTs. The developed biosensor was applied to the direct determination of 5-HT concentrations in undiluted healthy control and Internet gaming disorder serum samples. The results were verified by comparison with those from liquid chromatography-mass spectrometric analyses.

Keywords Serotonin · Serotonin-specific aptamer · Tyrosinase · Voltammetric biosensor · Internet gaming disorder · Single-walled carbon nanotubes

Introduction

Internet gaming disorder (IGD) which has a distinct characteristic of excessive and uncontrolled gaming behavior [1] becomes a social problem because more people including adolescents are exposed to a high risk of indulging in internet games and further resulting in IGD, while it has been shown that IGD is related to increased impulsivity and highly comorbid with depression and social phobia [2]. Lee et al. previously demonstrated that IGD is related to the dysregulation of serotonin (5-hydroxytryptamine, 5-HT) [3], a well-known monoamine neurotransmitter which plays an important role in regulating various physiological functions including appetite, mood, sexuality, obesity, and sleep [4–7]. 5-HT was also reported to be associated with depressive mood and anxiety as well as impulsivity [8]. While there are some studies to explore the role of 5-HT in IGD [2], the sensing of 5-HT level in biofluids with IGD has not been reported yet. Therefore, it is worthwhile to develop a feasible method for detection of 5-HT in human serum or plasma samples associated with IGD.

Conventional detection methodologies including radioimmunoassay [9], high-performance liquid chromatography [10], capillary electrophoresis [11], and spectrophotometry [12] have been employed for 5-HT which often require complicated sample pretreatment, expensive instruments, and tedious processes, whereas chemiluminescence, fluorescence, and electrochemical biosensors offering a simple and

✉ Ji Eun Lee
jelee9137@kist.re.kr

✉ Hye Jin Lee
hyejinlee@knu.ac.kr

[1] Department of Chemistry and Green-Nano Materials Research Center, Kyungpook National University, 80 Daehakro, Buk-gu, Daegu-city 41566, Republic of Korea

[2] Center for Theragnosis, Biomedical Research Division, Korea Institute of Science and Technology, 5 Hwarang-ro 14-gil, Seongbuk-gu, Seoul 02792, Republic of Korea

[3] Department of Psychiatry, SMG-SNU Boramae Medical Center, 20 Boramae-ro 5-gil, Dongjak-gu, Seoul 07061, Republic of Korea

[4] Environmental Fate & Exposure Research Group, Korea Institute of Toxicology (KIT), Jinju, Gyeongsangnam-do 52834, Republic of Korea

inexpensive fabrication process alongside high selectivity and sensitivity have been reported [13–16]. Among these, electrochemical biochip sensors have been most widely used and a list of electrochemical biosensing platforms for 5-HT are summarized in Table S1; for example, an electrochemical sensor using reduced graphene oxide and silver selenide composite self-assembled on glassy carbon electrode (GCE) provided a linearity region from 0.1 to15 μM having a limit of detection (LOD) value of 29.6 nM for 5-HT [15]. Further improvements in the selectivity alongside sensitivity toward 5-HT were made from integration of biorecognition elements such as DNA aptamer into electrochemical sensing surface [16].

In the current study, we demonstrate for the first time a highly selective and sensitive voltammetric biosensor featuring poly(diallyldimethylammonium)-wrapped oxidized single-walled carbon nanotubes (PDDA-oSWCNTs) in conjunction with 5-HT-specific aptamer and tyrosinase (Tyr) onto a screen printed carbon electrode (SPCE) for 5-HT in buffer and clinical serum samples. A simple layer-by-layer (LbL) assembly process of alternating the oppositely charged molecules was used instead of covalent attachment; a positively charged PDDA-oSWCNTs and a negatively charged 5-HT aptamer were alternately assembled onto a carboxylic acid-terminated monolayer modified gold nanoparticles (AuNPs) deposited SPCE followed by the adsorption of Tyr as the last layer. The combined use of DNA aptamer, Tyr, and PDDA-oSWCNTs was essential for constructing our sensor; an aptamer sequence specific to 5-HT was used for not only providing negatively charged surface but also improving the selectivity of our sensor. As a comparison, a negatively charged double-stranded DNA (dsDNA) with random sequences was employed instead of 5-HT aptamer. The PDDA was also employed in LbL assembly to offer not only a positively charged layer but also biocompatibility; polyaniline could be used but requires an organic solvent such as N,N-dimethylformamide [17] for LbL fabrication resulting in destroying an adhesion layer in SPCE. Furthermore, SWCNTs were used to enlarge the active surface area with an excellent electrical conductivity, which have been frequently employed for building electrochemical biosensors [18]. Lastly, the role of Tyr was to increase the selectivity where the hydroxyl group in 5-HT in contact with Tyr will be selectively electrocatalyzed to generate oxidative peak responses. Such an LbL assembly approach to introduce sensing compartment including enzymes, DNAs, metallic NPs, carbon allotropes, and polyelectrolytes has previously proven to be a promising tool for sensitive sensing of metabolites, proteins, and other targets [19–21]. Our biosensor was fully optimized for cyclic and differential pulse voltammetric analyses of different concentrations of 5-HT and further applied to the direct measurement of native 5-HT concentrations in undiluted healthy control (HC) and IGD serum samples. Liquid chromatography-mass spectrometry (LC-MS) analyses of 5-HT in the HC and IGD serum samples were also pursued for verification of the results of LbL sensor.

Experimental section

Materials and clinical samples

Materials including purified HIPCO SWCNTs (Unidym), Tyr from mushroom (7164 U/mg, isoelectric point of 4.7, Sigma-Aldrich), PDDA (35 wt.% in H_2O, Sigma-Aldrich), 5′-amine modified DNA aptamer specific to 5-HT of which sequence is 5′-NH_2-CTC TCG GGA CGA CTG GTA GGC AGA TAG GGG AAG CTG ATT CGA TGC GTG GGT CGT CCC-3′ [16] (Integrated DNA Technologies), and human normal serum (HNS, Sigma-Aldrich) were used as received. HC and IGD serum samples used in the current study were approved by the Institutional Review Board of SMG-SNU Boramae Medical Center (IRB No. 16-2014-139). It must be mentioned that all serum samples for electrochemical measurements were used as received without any pretreatment. Full details on materials and clinical samples are provided in the Supplementary Information.

Fabrication of LbL biosensor and electrochemical measurements

The fabrication process of LbL biosensor for 5-HT is shown in Fig. 1a. A disposable customized SPCE chip (Daeyoungsilk Co. Ltd., Republic of Korea) configuring an Ag/AgCl reference, a carbon counter, and a carbon working electrode (surface area = 28 mm^2) was used. AuNPs were first electrodeposited onto a SPCE surface using a chronoamperometric method [20] by immersing SPCE into 0.5 mM $HAuCl_4$ in 0.5 M H_2SO_4 with a constant potential 0.18 V under stirring followed by rinsing with water. The air-dried chip was immediately immersed into 20 mM ethanolic mercaptopropionic acid (MPA) solution overnight at room temperature to form a carboxylic acid-terminated monolayer. After rinsing sensor chip with ethanol and water, the LbL assembly process via electrostatic interaction underwent by alternatively dropping a 20-μL aliquot of PDDA-oSWCNTs following a procedure reported in literature [22] (see further details in Electronic Supplementary Material) and a 10-μL aliquot of 1 μM 5-HT aptamer on the MPA modified AuNPs-SPCE for 20 min. The surface assembled layers were confirmed via monitoring the tubular diameter of about 10 nm for oSWCNTs increased up to 50 nm when sequentially interacting with PDDA and 5-HT aptamer as seen in field emission-transmission electron microscope images (FE-TEM, Fig. S1) coupled with the presence of P element from energy dispersive spectroscopy analyses (EDS) (Table S2). The processes were repeatedly continued to achieve the optimal number of layers. The final layer of

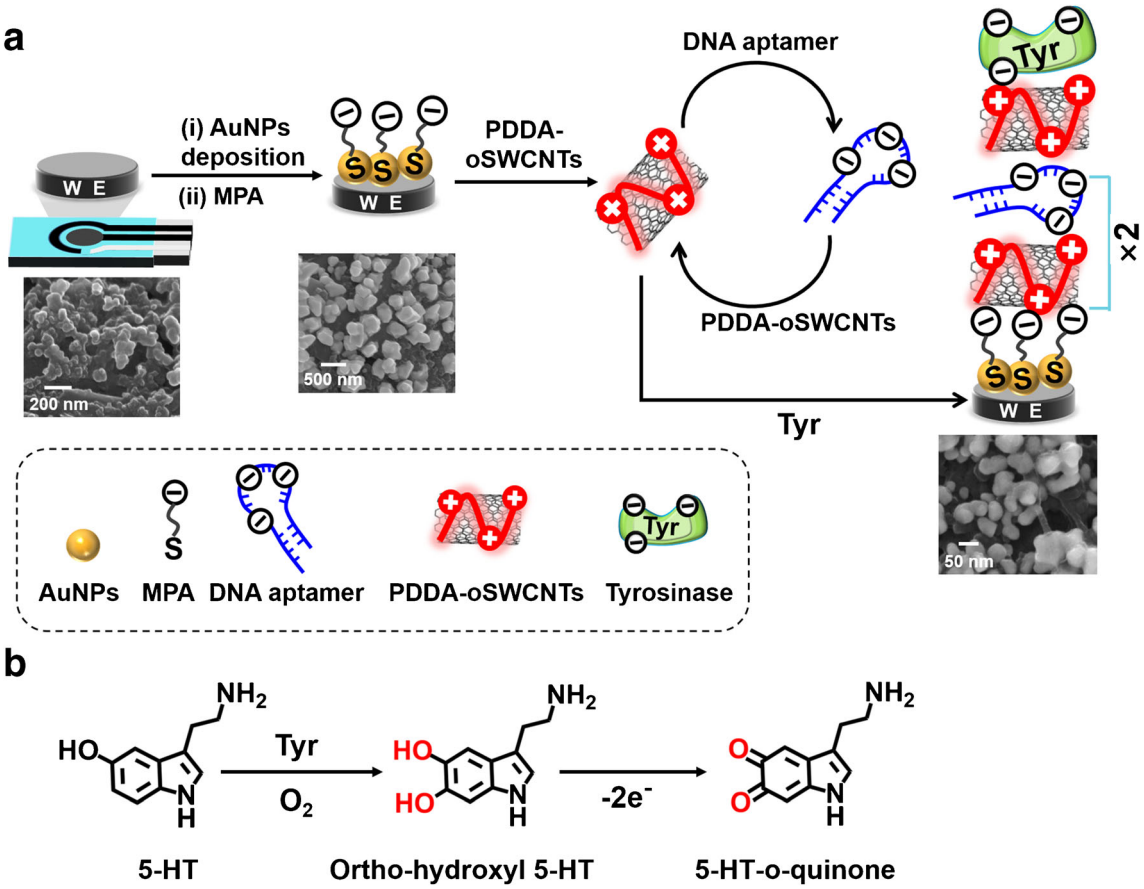

Fig. 1 **a** Schematic showing the preparation of 5-HT selective LbL biosensor composed of SPCE-AuNPs-MPA-(PDDA-oSWCNTs-5-HT aptamer)$_2$-PDDA-oSWCNTs-Tyr. **b** A brief reaction scheme for the catalysis of 5-HT and Tyr followed by the electro-oxidation of ortho-hydroxyl 5-HT

LbL biosensor was configured by exposing a 10-μL aliquot of 3 mg/mL Tyr solution to the electrode surface and incubated for 6 h at 4 °C. The prepared biosensors were finally rinsed with 10 mM phosphate-buffered saline solution (PBS, pH 7.0) and kept at 4 °C before any measurements. The surface morphology and elemental composition of LbL biosensors were characterized using FE-scanning electron microscopy (FE-SEM, a Hitachi SU8220 model) and X-ray photoelectron spectroscopy (XPS, Thermo Fisher NEXSA model), respectively. Electrochemical experiments were performed with a computer-controlled potentiostat (Autolab PGSTAT128N) connected with General Purpose Electrochemical system (GPEs) program (version 4.9).

Results and discussion

Voltammetric detection of 5-HT

The strategy to determine the concentrations of 5-HT in both buffer and serum sample solutions using our developed sensor is the combined use of 5-HT-specific aptamer and Tyr alongside oSWCNTs wrapped with polyelectrolytes for improving selectivity and sensitivity, respectively. A double bilayer of a positively charged PDDA-oSWCNTs and negatively charged 5-HT-specific aptamer on MPA modified AuNPs-SPCE chip with the Tyr as a final top layer, namely SPCE-AuNPs-MPA-(PDDA-oSWCNTs-5-HT aptamer)$_2$-PDDA-oSWCNTs-Tyr, was used to monitor the selective electrocatalytic reaction with 5-HT to produce ortho-hydroxyl 5-HT (see Fig. 1a). CV and DPV responses of the further electro-oxidation of ortho-hydroxyl 5-HT to 5-HT-o-quinone were directly correlated with the quantitative analyses of 5-HT (Fig. 1b). The homogeneously packed SWCNTs layers on the electrode surface, which resulted in enlarging the electroactive surface area and facilitating faster electron transfer process, were confirmed using FE-SEM, XPS, cyclic voltammetry (CV), and electrochemical impedance spectroscopy measurements (relevant results and full discussion are addressed in the Electronic Supplementary Material).

A typical voltammetric response for the electrocatalysis of 5-HT by Tyr at various concentrations of 5-HT when using the LbL biosensor is shown in Fig. 2. No reduction peak was seen at all concentrations due to the irreversible oxidation of

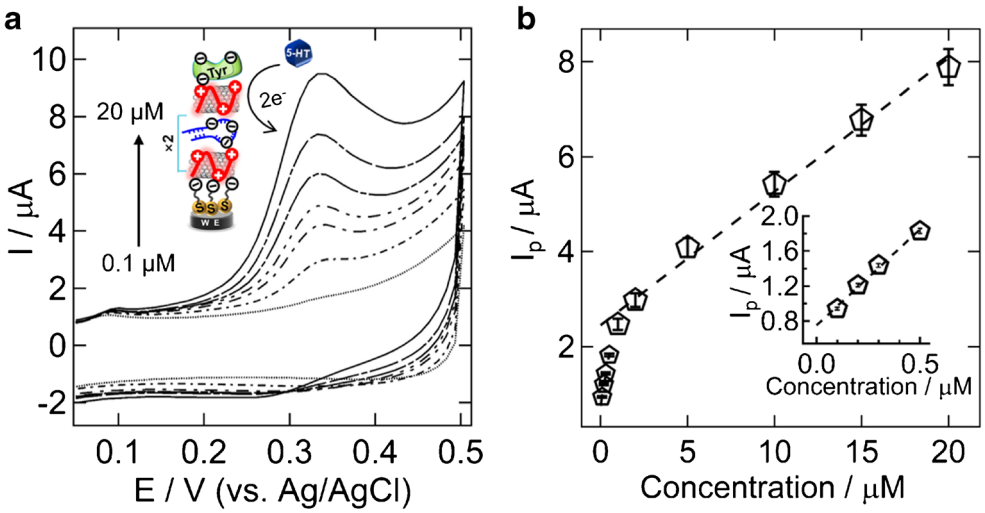

Fig. 2 Representative **a** CV data for the detection of various 5-HT concentrations (0.1, 1, 2, 5, 10, and 20 μM) using LbL biosensor consisting of SPCE-AuNPs-MPA-(PDDA-oSWCNTs-5-HT aptamer)$_2$-PDDA-oSWCNTs-Tyr in 10 mM PBS (pH 7.0). (⋯) is in the absence of 5-HT. Scan rate = 50 mV/s. **b** Calibration plots including some of data points taken from **a**. Inset in **b** shows the data points for the low concentration range of 5-HT

5-HT [23]. On the other hand, a peak-shaped current at ~0.33 V (vs. Ag/AgCl) resulting from the electro-oxidation of 5-HT to 5-HT-o-quinone linearly increased with respect to the 5-HT concentrations with two distinct dynamic regions from 0.1 to 0.5 and 1 to 20 μM with sensitivity (μA/μM/cm^2) values of 5.761 and 0.734, respectively (Fig. 2). The smaller sensitivity at high concentration range could be assigned to the internal resistance produced due to the limited diffusion of 5-HT as the concentration increased. The active sites could also be blocked with increased 5-HT concentration resulting in the saturation of oxidation current responses. This is a typical characteristic of surface-based sensing methods [24]. The estimated LOD was about 35 nM according to $3S_b/m$ criteria. The S_b is the standard deviation of the lowest detectable concentration and m is the corresponding calibration curve slope. In addition, the oxidative peak current was shifted more positively and increased versus the scan rate with a linear regression fit of y (μA) = 58.93x (V/s) + 0.92 (R^2 = 0.997), indicative of adsorption-controlled process (Fig. S6). The optimum adsorption time was measured as 60 s from cyclic voltammetric monitoring of the reaction of 5-HT and Tyr (Fig. S7). The superior oxidation peak current response from the LbL sensor at a fixed 5-HT concentration compared to those using differently modified sensors including only bare, direct attachment of Tyr on the electrode surface, and LbL biosensor in the absence of Tyr (Fig. S8) indicated that the combined use of Tyr and SWCNTs plays an important role in enhancing the sensitivity; for example, the peak current response at 0.33 V (vs. Ag/AgCl) for 10 μM 5-HT when using LbL biosensor (Fig. S8, iv) is 1.2 times higher than that using the sensor in the absence of Tyr (Fig. S8, iii). Such an enhancement in peak current due to the presence of enzyme can also be supported by previously published work on L-tyrosine detection [25, 26].

In order to further improve the sensitivity while lowering background current, a DPV technique was employed; the oxidative peak current at 0.29 V (vs. Ag/AgCl) associated with electrocatalysis of 5-HT similar to that of CV linearly increased depending on the 5-HT concentrations (Fig. 3a). The sensitivity for the range of 0.05–0.5 μM shows about 1.1 times higher and the LOD (2 nM) value is 10 times lower than that from the CV method (Fig. 3b). DPV performance of our LbL biosensor (i) for 5-HT compared to those using differently modified biosensors such as (ii) SPCE-AuNPs-MPA-Tyr and (iii) SPCE-AuNPs-MPA-(PDDA-5-HT aptamer)$_2$-PDDA-Tyr is summarized in Table S5. It is obvious that the LbL biosensor (i) shows the lowest LOD value in addition to the highest sensitivity for the dynamic range of 0.05–0.5 μM, which is 6 and 15 times higher than those modified electrodes without LbL modification (ii) and with only PDDA without SWCNTs as the positive layer for LbL fabrication (iii), respectively (Fig. S9). Such excellent sensing performance of 5-HT using the LbL biosensor could arise from the enlarged surface area with enhanced conductivity due to the presence of oSWCNTs assembled in the sensor when compared to that of using only PDDA. A neutrally charged and biocompatible polyethylene glycol (PEG) was also investigated as a sensing compartment instead of PDDA. The DPV response for 10 μM 5-HT when using PEG in LbL sensor was almost six times reduced compared to that of using PDDA, which confirms the necessity of positively charged polyelectrolyte layer (Fig. S10a). In addition, a negatively charged DNA with any sequences can be used instead of DNA sequences specific to 5-HT and it was observed that the use of randomly sequenced DNA in the sensor instead of using DNA aptamer specific to 5-HT slightly improved the sensitivity but reduced the selectivity which will be discussed in the next section.

Further comparison of the performance of our sensor to those from recently published research works listed in Table S1 revealed that the LOD and dynamic range of our biosensor for 5-HT detection are comparable or better than those of previously reported works utilizing multi-walled

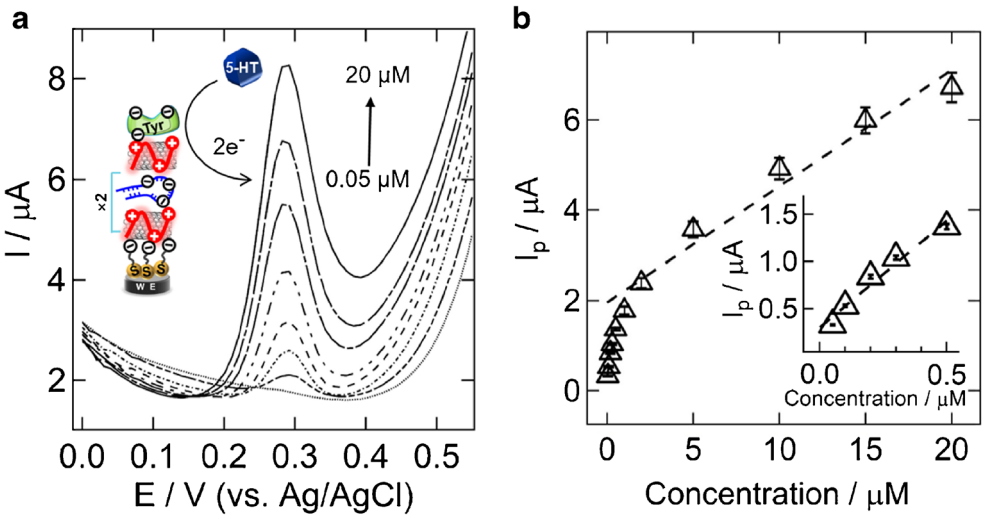

Fig. 3 Representative **a** DPV data for the detection of various 5-HT concentrations using LbL biosensor composed of SPCE-AuNPs-MPA-(PDDA-oSWCNTs-5-HT aptamer)$_2$-PDDA-oSWCNTs-Tyr in 10 mM PBS (pH 7.0). The 5-HT concentrations were 0.05, 0.2, 0.5, 2, 5, 10, and 20 μM. (····) is in the absence of 5-HT. A step potential of 10 mV, scan rate of 20 mV/s, pulse interval of 50 ms, and amplitude of 50 mV were used. **b** Calibration plots including data points taken from **a**. Inset in **b** shows the data points for the low concentration range of 5-HT

CNTs-chitosan-poly(m-aminobenzenesulfonic acid), AuNPs/Au nanorattles-reduced graphene (rGO), and rGO/Co_3O_4 modified GCE [23, 27, 28]. More importantly, the dynamic range of our LbL biosensor for 5-HT falls within clinically relevant serum concentration level from 0.48 to 1.33 μM [29].

Besides the sensitivity and LOD, the reproducibility, stability, reusability, and selectivity are also important compartments in the sensor used for clinical sample analyses. The relative standard deviation (RSD) value of seven electrodes was 3.3% obtained from measurements of DPV responses at a fixed concentration of 5-HT of 5 μM on seven individually prepared LbL biosensors under the same condition (see Fig. 4a). As for the stability of our LbL biosensor, the biosensor performance retained about 81% of its initial activity with an RSD value of 5.9% after 9 days (Fig. 4b) when the sensor was stored in a humid Petri dish in the dark at 4 °C. The reusability was also examined by recording DPV response of 10 μM 5-HT repeatedly with a single sensor via washing it with PBS buffer followed by incubated with PBS buffer for 1 h in a dark and humidity chamber after each measurement. As we reused three times, the peak current value decreased about 40%, and then 70% after 4th usage due to possible loss of enzyme activity and electrode surface contamination (Fig. S10b).

The selectivity of the LbL biosensor was investigated using some interfering agents, which have similar structures to 5-HT and are known to be present in human serum samples (Fig. S11, i). These are glucose (Glu 10 mM), dopamine (DA 1 μM), epinephrine (EP 1 μM), tryptophan (TP 40 μM), and tyrosine (Ty 50 μM). The concentration of each interfering agent was set to be higher or similar level in human serum [25, 30–33]. The DPV peak current recoveries of 5-HT only and 5-HT with the addition of above interfering reagents were evaluated. A less than 4% increase in the recovery was observed for each solution containing either Glu, DA, EP, or Ty. In the presence of TP, around 11% decrease was seen, which could result from the competitive reaction of TP with 5-HT toward Tyr. Interestingly, the LbL biosensor incorporated with a dsDNA layer instead of 5-HT-specific DNA aptamer was found to be more prone to be affected by the interfering

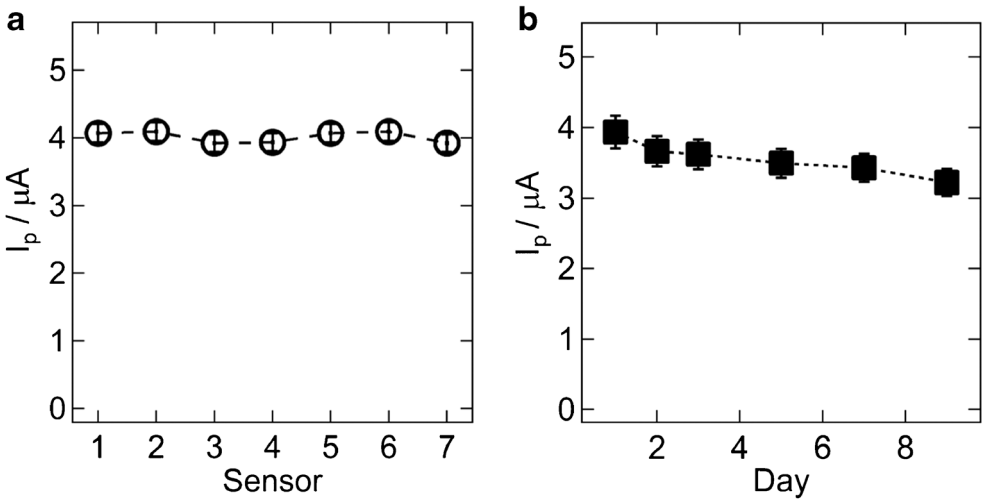

Fig. 4 **a** Reproducibility and **b** stability tests of LbL biosensor for 5-HT at a fixed concentration of 5 μM 5-HT in 10 mM PBS

compounds, for example, Glu, TP, and Ty with a significant decrease of 6%, 25%, and 22%, respectively (Fig. S11, ii). This implies that the use of 5-HT-specific aptamer layer in the LbL biosensor helped enhance the selectivity for detection of 5-HT.

Analyses of 5-HT in clinical samples

Confirmed the clinically relevant level of selectivity and sensitivity of our LbL biosensor, native 5-HT concentrations in undiluted pooled HC and IGD samples from a local medical center using the LbL biosensor were determined for exploring potential applicability of IGD diagnosis. DPV responses of two different sets of undiluted pooled HC and IGD serum samples followed by spiking a series of known 5-HT concentrations ranging from 1 to 6 μM into the samples were measured and analyzed with a well-known standard addition method. Considering background effects due to the coexistence of different metabolites and 5-HT in the serum samples, each raw DPV data was baseline-corrected using OriginLab software and then used for 5-HT analyses.

The oxidative DPV peak current corrected by baseline for both the pooled HC and IGD serum samples (1st set) increased linearly as a function of the spiked known concentrations (1–6 μM) of 5-HT (see Fig. 5a and b, respectively). The resulting linear fit equations of the pooled HC and IGD samples (1st set) in Fig. 5c were y (μA) = 0.19x (μM) + 0.70 and y (μA) = 0.24x (μM) + 0.97, respectively. By substituting the baseline-corrected peak current (μA) values of 0.82 and 1.16 for the pooled HC and IGD serum samples only into the linear fit equation (1st set), the native 5-HT concentrations were then estimated as 0.63 ± 0.03 and 0.79 ± 0.04 μM, respectively. It should be mentioned that the shift of peak potential and different linear ranges in undiluted serum samples could be due to the severe matrix effect leading to a reduced sensitivity of 5-HT compared to that of buffer (0.48 μA/μM for 5-HT concentrations ranging from 1 to 5 μM). For example, matrix components such as ions, hormones, and amino acids present in undiluted serum solutions could affect the electrochemical sensing results of 5-HT due to altered ion strength and close oxidation peak potential while proteins could interact with the sensor surface and hinder the accessibility of the analyte [34, 35]. In addition, the high viscosity of undiluted human serum has an influence on the diffusion flux of 5-HT to the electrode surface. These problems could be resolved by modifying electrode surface with anti-fouling nanomaterials such as self-assembled monolayers and sample pretreatment processes [36]. Our LbL biosensor was further applied to analyze another set of pooled HC and IGD samples (2nd set, see Fig. S12) with the same approach and the 5-HT concentrations evaluated were 0.58 ± 0.04 and 0.74 ± 0.05 μM, respectively, from HC and IGD samples (2nd set).

Our LbL sensing results from the two different sets of pooled HC and IGD samples were finally verified via comparing those using LC-MS technique, and the summary is listed in Table 1. The measured 5-HT concentration values of the pooled HC and IGD serum samples using the LbL biosensor were generally in good agreement with those obtained from the LC-MS analyses; slightly higher concentration values estimated from the LbL sensor for all serum samples. The divergence could be due to (i) systematic error caused by imperfect calibration and environment interference and (ii) matrix effects in undiluted serum samples (e.g., DA, Glu, TP interferents) resulting in the overestimation of 5-HT in electrochemical sensing. Nevertheless, it must be noted that the measured concentrations levels from both LbL biosensor and LC-MS analyses showed the 5-HT levels were higher in IGD samples than in HCs, which evidently demonstrates that the concentrations of the 5-HT are significantly associated with the IGD in serum samples. In addition, the 5-HT

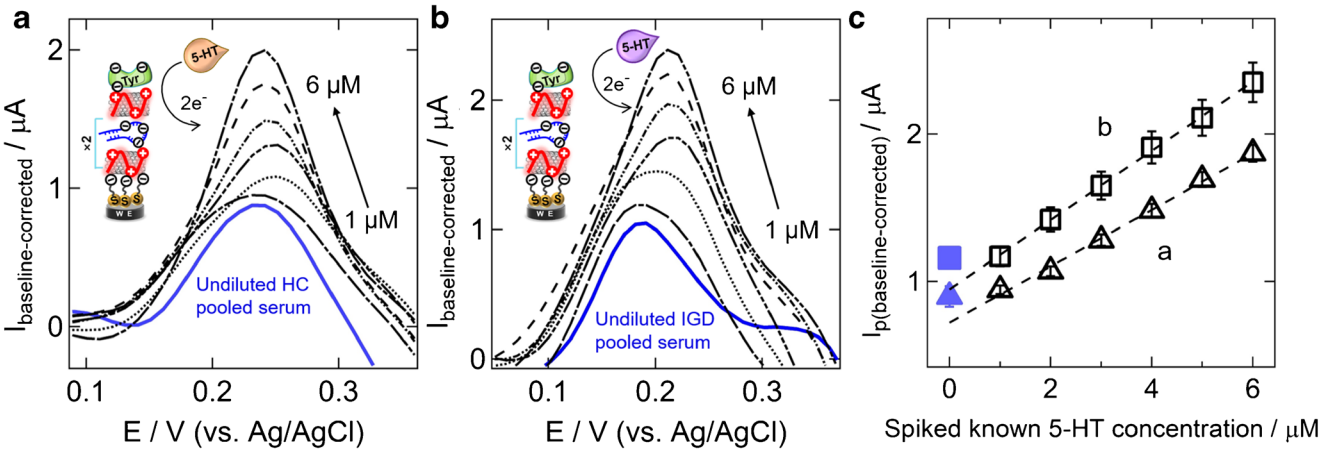

Fig. 5 Representative baseline-corrected DPV responses for 5-HT concentrations ranging from 1 to 6 μM in undiluted **a** pooled HC and **b** IGD serum samples using LbL biosensor. The solid curve in **a** and **b** is the data acquired from serum itself without spiked 5-HT. The same DPV parameters as described in Fig. 3 were used. **c** Calibration plots corresponding to **a** and **b** with pooled HC and IGD serum samples (1st set), respectively. (▲) and (■) represent the pooled HC and IGD serum samples only, respectively

Table 1 Summary of 5-HT concentrations in undiluted pooled HC and IGD serum samples using LbL biosensor and LC-MS analyses

Sample		$C_{5\text{-HT}}$/μM (biosensor)	$C_{5\text{-HT}}$/μM (LC-MS)
HC sample	1st	0.63 ± 0.03	0.49 ± 0.03
	2nd	0.58 ± 0.04	0.52 ± 0.05
IGD sample	1st	0.79 ± 0.04	0.74 ± 0.04
	2nd	0.74 ± 0.05	0.70 ± 0.03

concentration levels in the pooled HC samples were comparable to that obtained from HNS (0.50 ± 0.04 μM, see Fig S13). However, the LbL biosensor still needs challenging improvements including the limited storage stability (<10 days) and reusability (1 or 2 times), alongside the selectivity explicitly distinguishing the peak potentials between the interfering agents of ascorbic acid and 5-HT.

Conclusions

An LbL assembled voltammetric biosensor consisting of alternating layers of PDDA-oSWCNTs, and 5-HT aptamer, followed by the final layer of Tyr on AuNPs deposited SPCE was successfully developed for the direct analyses of 5-HT concentrations in buffer and undiluted HC and IGD serum samples. The use of both Tyr and 5-HT aptamer contributed to the enhancement of sensitivity and selectivity toward detection of 5-HT, whereas the oSWCNTs were capable of improving the sensitivity of the LbL biosensor. Such an improved sensitivity is superior to some of the recently published methods for 5-HT detection including the use of carbon, metallic, and/or polymeric nanocomposites as a performance-enhancing tool (Table S1). Moreover, the results from our LbL biosensors were in good agreement with those of LC-MS of the 5-HT analyses in the pooled HC and IGD serum samples, which clearly shows that the concentrations of the 5-HT are significantly related to the IGD and that our biosensor for 5-HT can be used as a potential diagnostic method for 5-HT indicative of IGD.

Supplementary Information The online version contains supplementary material available at https://doi.org/10.1007/s00604-021-04798-x.

Funding This work was supported by the National Research Foundation of Korea (NRF) grant funded by the Korea government (Ministry of Science and ICT, MSIT) (grant number: NRF-2020R1A4A1018393).

Compliance with ethical standards

Conflict of interest The authors declare no competing interests.

References

1. Kuss DJ (2013) Internet gaming addiction: current perspectives. Psychol Res Behav Manag 6:125–137. https://doi.org/10.2147/PRBM.S39476
2. Han DH, Hyun GJ, Park JH, Renshaw PF (2016) Internet gaming disorder, Neuropathology of drug addictions and substance misuse. Academic Press, pp 955–961
3. Lee YS, Han DH, Yang KC, Daniels MA, Na C, Kee BS, Renshaw PF (2008) Depression like characteristics of 5HTTLPR polymorphism and temperament in excessive internet users. J Affect Disord 109:165–169. https://doi.org/10.1016/j.jad.2007.10.020
4. Yadav VK, Oury F, Suda N, Liu ZW, Gao XB, Confavreux C, Klemenhagen KC, Tanaka KF, Gingrich JA, Guo XE, Tecott LH, Mann JJ, Hen R, Horvath TL, Karsenty G (2009) A serotonin-dependent mechanism explains the leptin regulation of bone mass, appetite, and energy expenditure. Cell 138:976–989. https://doi.org/10.1016/j.cell.2009.06.051
5. Haahr ME, Rasmussen PM, Madsen K, Marner L, Ratner C, Gillings N, Baare WFC, Knudsen GM (2012) Obesity is associated with high serotonin 4 receptor availability in the brain reward circuitry. Neuroimage 61:884–888. https://doi.org/10.1016/j.neuroimage.2012.03.050
6. Sanghavi BJ, Wolfbeis OS, Hirsch T, Swami NS (2015) Nanomaterial-based electrochemical sensing of neurological drugs and neurotransmitters. Microchim Acta 182:1–41. https://doi.org/10.1007/s00604-014-1308-4
7. Khoshnevisan K, Maleki H, Honarvarfard E, Baharifar H, Gholami M, Faridbod F, Larijani B, Faridi Majidi R, Khorramizadeh MR (2019) Nanomaterial based electrochemical sensing of the biomarker serotonin: a comprehensive review. Microchim Acta 186:49. https://doi.org/10.1007/s00604-018-3069-y
8. Lesch KP, Merschdorf U (2000) Impulsivity, aggression, and serotonin: a molecular psychobiological perspective. Behav Sci Law 18:581–604. https://doi.org/10.1002/1099-0798(200010)18:5<581::aid-bsl411>3.0.co;2-l
9. Manz B, Kosfeld H, Harbauer G, Grill HJ, Pollow K (1985) Radioimmunoassay of human serum serotonin. J Clin Chem Clin Biochem 23:657–662. https://doi.org/10.1515/cclm.1985.23.10.657
10. Zhang J, Jaquins-Gerstl A, Nesbitt KM, Rutan SC, Michael AC, Weber SG (2013) In vivo monitoring of serotonin in the striatum of freely moving rats with one minute temporal resolution by online microdialysis-capillary high-performance liquid chromatography at elevated temperature and pressure. Anal Chem 85:9889–9897. https://doi.org/10.1021/ac4023605
11. Hsieh MM, Chang HT (2005) Discontinuous electrolyte systems for improved detection of biologically active amines and acids by capillary electrophoresis with laser-induced native fluorescence detection. Electrophoresis 26:187–195. https://doi.org/10.1002/elps.200406123
12. Ramon-Marquez T, Medina-Castillo AL, Fernandez-Gutierrez A, Fernandez-Sanchez JF (2016) A novel optical biosensor for direct and selective determination of serotonin in serum by solid surface-room temperature phosphorescence. Biosens Bioelectron 82:217–223. https://doi.org/10.1016/j.bios.2016.04.008
13. Israël M (2003) A chemiluminescent serotonin assay. Neurochem Int 42:215–220. https://doi.org/10.1016/S0197-0186(02)00095-5
14. Wang G, Geng L (2005) Statistical and generalized two-dimensional correlation spectroscopy of multiple ionization states. Fluorescence of neurotransmitter serotonin. Anal Chem 77:20–29. https://doi.org/10.1021/ac0492362
15. Selvam SP, Yun K (2020) A self-assembled silver chalcogenide electrochemical sensor based on rGO-Ag_2Se for highly selective

detection of serotonin. Sensors Actuators B Chem 302:127161. https://doi.org/10.1016/j.snb.2019.127161
16. Nakatsuka N, Yang KA, Abendroth JM, Cheung KM, Xu X, Yang H, Zhao C, Zhu B, Rim YS, Yang Y, Weiss PS, Stojanović MN, Andrews AM (2018) Aptamer-field-effect transistors overcome Debye length limitations for small-molecule sensing. Science 362: 319–324. https://doi.org/10.1126/science.aao6750
17. Ghobashy MM, Alkhursani SA, Madani M (2018) Radiation-induced nucleation and pH-controlled nanostructure shape of polyaniline dispersed in DMF. Polym Bull 75:5477–5492. https://doi.org/10.1007/s00289-018-2336-8
18. Iost RM, Crespilho FN (2012) Layer-by-layer self-assembly and electrochemistry: applications in biosensing and bioelectronics. Biosens Bioelectron 31:1–10. https://doi.org/10.1016/j.bios.2011.10.040
19. Lee Y-G, Lee HJ, Jang A (2017) Amperometric bromate-sensitive sensor via layer-by-layer assembling of metalloporphyrin and poly-electrolytes on carbon nanotubes modified surfaces. Sensors Actuators B Chem 244:157–166. https://doi.org/10.1016/j.snb.2016.12.114
20. Karim MN, Lee JE, Lee HJ (2014) Amperometric detection of catechol using tyrosinase modified electrodes enhanced by the layer-by-layer assembly of gold nanocubes and polyelectrolytes. Biosens Bioelectron 61:147–151. https://doi.org/10.1016/j.bios.2014.05.011
21. Ibáñez-Redín G, Joshi N, do Nascimento GF, Wilson D, Melendez ME, Carvalho AL et al (2020) Determination of p53 biomarker using an electrochemical immunoassay based on layer-by-layer films with $NiFe_2O_4$ nanoparticles. Microchim Acta 187:619. https://doi.org/10.1007/s00604-020-04594-z
22. He P, Bayachou M (2005) Layer-by-layer fabrication and characterization of DNA-wrapped single-walled carbon nanotube particles. Langmuir 21:6086–6092. https://doi.org/10.1021/la050581b
23. Ran G, Chen CN, Gu C (2015) Serotonin sensor based on a glassy carbon electrode modified with multiwalled carbon nanotubes, chitosan and poly(p-aminobenzenesulfonate). Microchim Acta 182: 1323–1328. https://doi.org/10.1007/s00604-015-1454-3
24. Karikalan N, Karthik R, Chen SM, Karuppiah C, Elangovan A (2017) Sonochemical synthesis of sulfur doped reduced graphene oxide supported CuS nanoparticles for the non-enzymatic glucose sensor applications. Sci Rep 7:2494. https://doi.org/10.1038/s41598-017-02479-5
25. Apetrei IM, Apetrei C (2019) Development of a novel biosensor based on tyrosinase/platinum nanoparticles/chitosan/graphene lanostructured layer with applicability in bioanalysis. Materials 12:1009. https://doi.org/10.3390/ma12071009
26. Kanchana P, Lavanya N, Sekar C (2014) Development of amperometric L-tyrosine sensor based on Fe-doped hydroxyapatite nanoparticles. Mater Sci Eng C 35:85–91. https://doi.org/10.1016/j.msec.2013.10.013
27. Mahato K, Purohit B, Bhardwaj K, Jaiswal A, Chandra P (2019) Novel electrochemical biosensor for serotonin detection based on gold nanorattles decorated reduced graphene oxide in biological fluids and *in vitro* model. Biosens Bioelectron 142:111502. https://doi.org/10.1016/j.bios.2019.111502
28. Shahid MM, Rameshkumar P, Numan A, Shahabuddin S, Alizadeh M, Khiew PS, Chiu WS (2019) A cobalt oxide nanocubes interleaved reduced graphene oxide nanocomposite modified glassy carbon electrode for amperometric detection of serotonin. Mater Sci Eng C 100:388–395. https://doi.org/10.1016/j.msec.2019.02.107
29. Babaei A, Taheri AR (2013) Nafion/$Ni(OH)_2$ nanoparticles-carbon nanotube composite modified glassy carbon electrode as a sensor for simultaneous determination of dopamine and serotonin in the presence of ascorbic acid. Sensors Actuators B Chem 176:543–551. https://doi.org/10.1016/j.snb.2012.09.021
30. Abboud I, Lerolle N, Urien S, Tadie JM, Leviel F, Fagon JY, Faisy C (2009) Pharmacokinetics of epinephrine in patients with septic shock: modelization and interaction with endogenous neurohormonal status. Crit Care 13:R120. https://doi.org/10.1186/cc7972
31. Si Y, Park YE, Lee JE, Lee HJ (2020) Nanocomposites of poly(L-methionine), carbon nanotube-graphene complexes and Au nanoparticles on screen printed carbon electrodes for electrochemical analyses of dopamine and uric acid in human urine solutions. Analyst 145:3656–3665. https://doi.org/10.1039/c9an02638j
32. Song MJ, Kim S, Ki Min N, Jin JH (2014) Electrochemical serotonin monitoring of poly(ethylenedioxythiophene):poly(sodium 4-styrenesulfonate)-modified fluorine-doped tin oxide by predeposition of self-assembled 4-pyridylporphyrin. Biosens Bioelectron 52:411–416. https://doi.org/10.1016/j.bios.2013.08.040
33. Wenninger J, Meinitzer A, Holasek S, Schnedl WJ, Zelzer S, Mangge H, Herrmann M, Enko D (2019) Associations between tryptophan and iron metabolism observed in individuals with and without iron deficiency. Sci Rep 9:14548. https://doi.org/10.1038/s41598-019-51215-8
34. Masson JF (2020) Consideration of sample matrix effects and "biological" noise in optimizing the limit of detection of biosensors. ACS Sens 5:3290–3292. https://doi.org/10.1021/acssensors.0c02254
35. Sun J, Liu Y (2018) Matrix effect study and immunoassay detection using electrolyte-gated graphene biosensor. Micromachines 9:142. https://doi.org/10.3390/mi9040142
36. Lin PH, Li BR (2020) Antifouling strategies in advanced electrochemical sensors and biosensors. Analyst 145:1110–1120. https://doi.org/10.1039/c9an02017a